



Pergamon

Bioorganic & Medicinal Chemistry 10 (2002) 2511–2526

BIOORGANIC &
MEDICINAL
CHEMISTRY

Design, Synthesis and QSAR Studies on *N*-Aryl Heteroarylisopropanolamines, a New Class of Non-Peptidic HIV-1 Protease Inhibitors

Roberto Di Santo,^a Roberta Costi,^a Marino Artico,^{a,*} Silvio Massa,^b Rino Ragno,^c Garland R. Marshall^{d,*} and Paolo La Colla^e

^a*Istituto Pasteur-Fondazione Cenci Bolognetti, Dipartimento di Studi Farmaceutici, Università degli Studi di Roma 'La Sapienza', P.le A. Moro 5, I-00185 Roma, Italy*

^{bb}*Dipartimento Farmaco Chimico Tecnologico, Università degli Studi di Siena, Via A. Moro 5, San Miniato, I-53100 Siena, Italy*

^c*Dipartimento di Studi di Chimica e Tecnologia delle Sostanze Biologicamente Attive, Università degli Studi di Roma 'La Sapienza', P.le Aldo Moro 5, I-00185 Roma, Italy*

^d*Center for Molecular Design, Washington University, St. Louis, MO 63110, USA*

^e*Dipartimento di Biologia Sperimentale, Sezione di Microbiologia, Università degli Studi di Cagliari, Cittadella Universitaria, I-09042 Monserrato, Cagliari, Italy*

Received 23 October 2001; accepted 2 April 2002

Abstract—A series of *N*-aryl heteroarylisopropanolamines in which an indole or a 3-arylpyrrole moiety was linked to an aryl group through an isopropanolamine linker, were designed and synthesized as potential anti-HIV-1-PR agents. Series was tested for their ability in blocking PR activity. As a rule, indole derivatives of class **1** exhibited more potency than pyrrole analogues of class **2** while *tert*-butylamide substituents increased anti-PR potency. In fact, bis *tert*-butylamide **1e** showed the highest activity with IC₅₀ = 25 μM. Even if not very potent, a simple class of anti-PR agents, with a facile synthetic pathway was discovered. QSAR studies on isopropanolamines **1** and **2** were performed in comparison with diarylbutanols, a new class of non peptidic anti-PR agents, recently discovered by Agouron Pharmaceuticals. QSAR and CoMFA models based on 30 diarylbutanols used as a training set were developed. The obtained models were used to investigate the binding mode of the newly synthesized derivatives **1** and **2**. The results of this study suggest that *N*-aryl heteroarylisopropanolamines bind to the PR active site similarly to the diarylbutanols of Agouron. © 2002 Elsevier Science Ltd. All rights reserved.

Introduction

The first approach to AIDS therapy utilized inhibitors of immunodeficiency virus type-1 reverse transcriptase enzyme (RT).¹ The rapid emergence of drug-resistant strains during AIDS clinical trials with HIV-1 RT inhibitors, due to the high levels of mutations and high replication levels of virus in vivo, led to targeting different viral enzymes such as HIV protease (PR) that plays a vital role in viral replicating cycle.²

PR is classified as an aspartic proteinase containing the typical Asp-Thr-Gly active-site sequence. The crystal structure of HIV-1 PR shows a dimer exhibiting exact

2-fold rotational C₂ symmetry with each monomer containing one of the catalytic aspartic acid residues.³ PR is essential for cleavage of the gag/pol polyprotein into viral structural proteins and enzymes during various stages of viral maturation. The ability of HIV protease to cleave phenylalanine(tyrosine)-proline peptide bonds makes PR unique in its substrate specificity as most proteolytic enzymes do not cleave on the N-terminal side of a prolyl residue.

Studies on peptidomimetic protease inhibitors led to the discovery of saquinavir, the first HIV protease inhibitor to undergo clinical evaluation.⁴ After saquinavir, a number of peptidomimetic derivatives were found to be very potent PR inhibitors (ritonavir,⁵ indinavir,⁶ amprenavir,⁷ nelfinavir⁸) and are currently used in clinical practice. Although PR inhibitors represented a major advance in the management of HIV disease, adverse side effects and viral resistance have encouraged

*Corresponding authors. Tel.: +39-06-446-2731; fax: +39-06-446-2731; e-mail: marino.artico@uniroma1.it (M. Artico). Tel.: +1-314-362-1567; fax: +1-314-362-0234; e-mail: garland@ibc.wustl.edu (G. Marshall)

research to develop PR inhibitors with different profiles of resistance to HIV strains. A further limitation of current PR inhibitors is their complexity and the concomitant arduous synthetic pathway with high costs of production. In order to overcome the above difficulties, it is desirable to identify new non-peptidic HIV PR inhibitors (PRI) of simpler structure. Up till now, only a few non-peptidic drugs, such as nelfinavir, DuPont Merck cyclic ureas⁹ or Parke-Davis dihydropyranones,¹⁰ reached trials, signifying the urgent need for new non-peptidic inhibitors.

A structural analysis of peptidic drugs such as saquinavir, nelfinavir, amprenavir,^{7,11} caused us to question whether the central isopropanolamine unit of the above substrate analogues was a binding determinant. Moreover, some diarylbutanols^{12,13} were recently reported by Agouron Pharmaceuticals to possess good anti-PR activity consistent with the hypothesis that two aryl moieties, through a four-atoms linker with carbinol unit mimicking the transition state, is a useful approach to design PR inhibitors.

Therefore, we designed and synthesized a series of *N*-aryl heteroarylisopropanolamines **1** and **2** reported in Figure 1 in which an indole ring, mimicking the aminoindane group of indinavir, was linked to an aryl moiety through an isopropanolamine group (structures **1**). The indole was also replaced with its open form represented by 3-arylpyrrole (structures **2**) and a number of substituents on indole, arylpyrrole and aryl groups were tested to better define the SAR in this series. In particular, *tert*-butylcarboxamide groups were linked in the 2 or 3-position of the aromatic or hetero-

aromatic rings, being typical moieties shown to improve anti-PR activity (i.e., saquinavir, indinavir, nelfinavir and diarylbutanols).

As the three-dimensional (3-D) structure of HIV-1-PR bound to some diarylbutanols¹³ was available, an important goal of our study was to determine whether or not the new PRIs share a common binding mode with Agouron's reference compounds. To reach this objective, we have undertaken classical and three-dimensional 3-D quantitative structure–activity relationships (QSARs) to derive statistical models using a training set of a series of diarylbutanols.^{12–14} The models obtained were then used as tools to evaluate binding modes of the new compounds (see Appendixes).

Chemistry

Isopropanolamines **1** and **2** were obtained as reported in Schemes 1–3. Indole derivatives **1** were synthesized by alkylation of ethyl indole-3-carboxylate or ethyl 5-chloroindole-3-carboxylate with epichloridrin in alkaline medium (K_2CO_3) and the oxiranyl derivatives **5** and **6** which formed, were reacted with methyl anthranilate at 90 °C to obtain isopropanolamines **1a** and **1d**. Finally, treatment of the latter compounds with *tert*-BuNH₂ and Al(CH₃)₃ gave a mixture of mono *tert*-butylamides **1b** and **1e** and bis *tert*-butylamides **1c** and **1f**, respectively (Scheme 1).

A similar synthetic route led to pyrrole derivatives **2a–q**. In fact, the appropriate pyrrole **7–10** was alkylated with

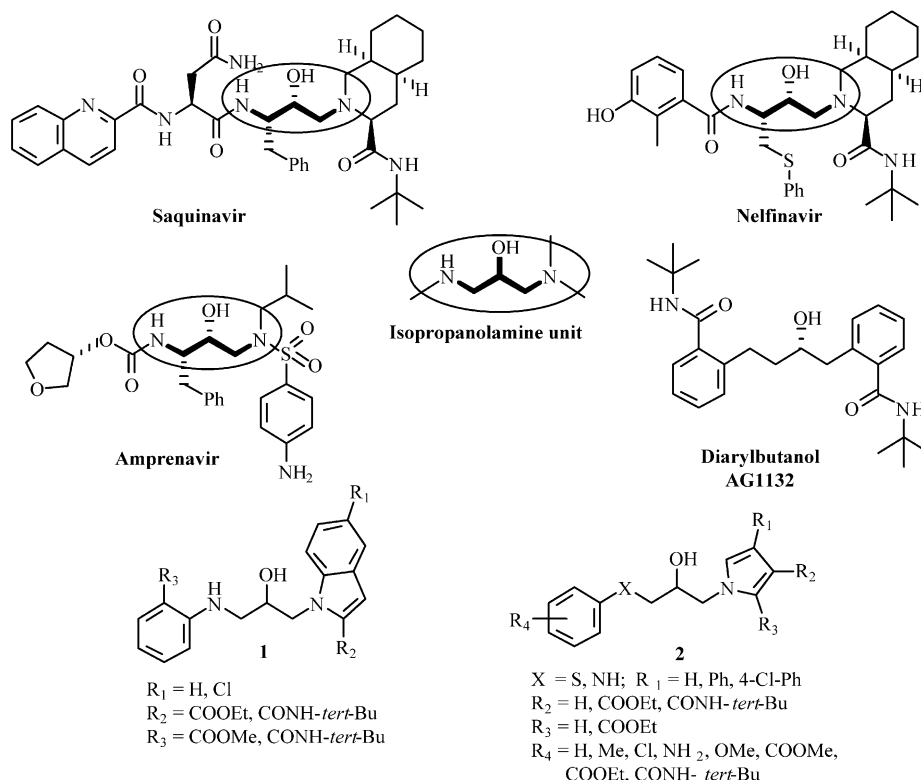
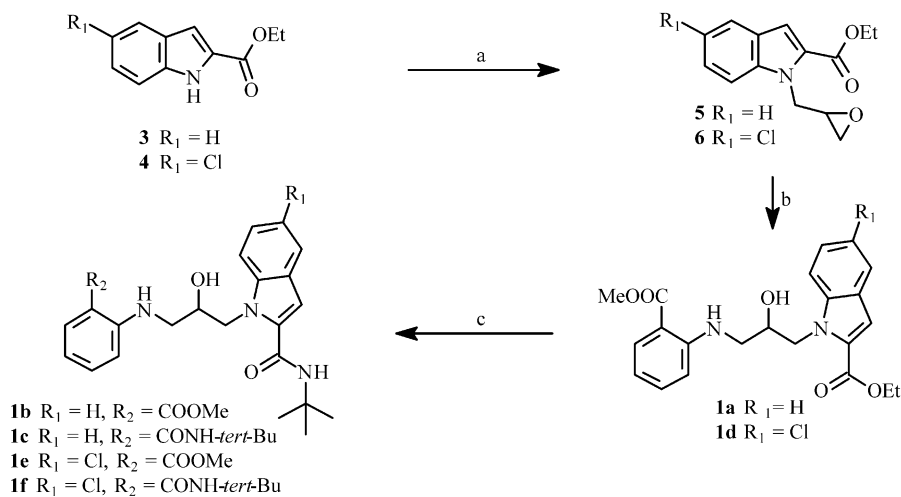
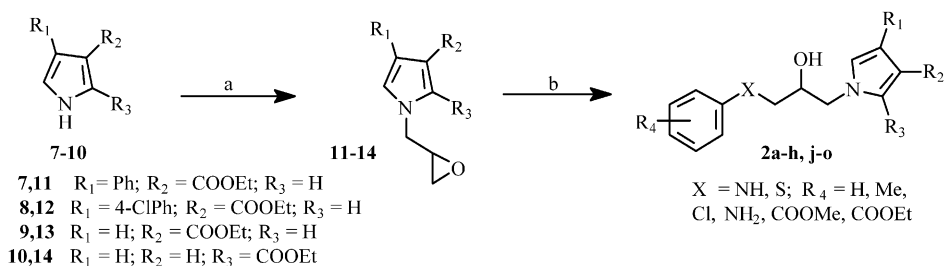


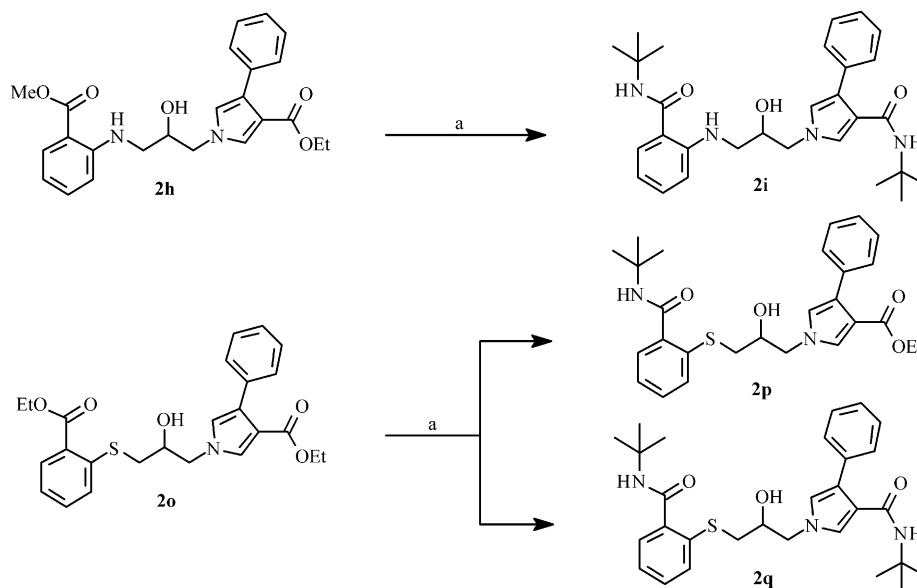
Figure 1. Newly synthesized anti-PR agents compared with known PR inhibitors.



Scheme 1. (a) Epichlorohydrin, K_2CO_3 ; (b) methylanthranilate, $90^\circ C$; (c) *tert*-butylamine, $Al(Me)_3$.



Scheme 2. (a) Epichlorohydrin, K_2CO_3 ; (b) substituted aniline or thiophenol, $90^\circ C$.



Scheme 3. (a) *tert*-Butylamine, $Al(Me)_3$.

epichloridrin using potassium carbonate as a catalyst and the oxiranylmethyl pyrroles **11–14** which formed, underwent ring opening by reaction with methyl anthranilate at $90^\circ C$ without solvent to afford **2a–h, j–m**. Similarly, arylthiopropansols **2n–o** were obtained by

reaction of oxirane **11** with the appropriate thiophenol in refluxing ethanol (Scheme 2).

Finally, diester **2o** was treated with $Al(CH_3)_3$ /*tert*- $BuNH_2$ complex to give a mixture of mono *tert*-butyla-

amide **2p** and bis *tert*-butylamide **2q**, while treatment of pyrrole derivative **2h** with the same reagent gave only bis *tert*-butylamide **2i** (Scheme 3).

Indole and pyrrole derivatives **3**, **4** and **7–10** used as starting materials, were synthesized either by annulation of tosylmethylisocyanide (TosMIC) with the appropriate Michael acceptor as already reported^{15,16} or by esterification of commercially available pyrrole-2-carboxylic acid and indole-2-carboxylic acid. The anti-HIV-1 PR activity and the cytotoxicity of the derivatives of classes **1** and **2** are reported in Table 1.

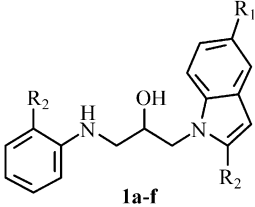
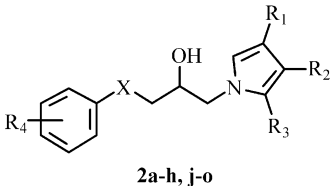
Molecular Modeling and QSAR Methods

All the computational work was performed on Silicon Graphics computers (O2 R10000 225 MHz). The measurements of biological activity used to develop the QSAR and 3-D QSAR were expressed as $(pIC_{50}) = -\log(IC_{50})$. To the derivatives that were found to be 'inactive' ($IC_{50} > 200 \mu M$), an activity value equal to 50% of that of the compound reported as the less active was arbitrarily assigned;¹⁷ for enantiomeric modeled compound of which no information of the actual IC_{50} value, half of the corresponding racemate inhibitory concentration was used.

The QSAR and 3-D QSAR were derived using as training set a series of diarylbutanols taken from the literature.^{12–14} The QSAR method used 3-D calculated parameters compiled by mean of the VALIDATE^{16,19} and VALIDATE II²⁰ procedures while the second method was a comparative molecular field analysis (CoMFA) as implemented in SYBYL.²¹

VALIDATE and VALIDATE II are hybrid approaches (QSAR and scoring functions) that make the maximal use of the three-dimensional information's from the 3-D coordinates of known ligand-receptor complexes. In this approach the contributions to the overall free energy variation upon complex formation were estimated by twenty-nine chemical and physical-chemical calculated parameters/scores, that were then correlated with the binding affinities (pK_i s or pIC_{50}). Due to the redundancy of some parameters, fractional factorial design (FFD) was used for variable selection as implemented in the program GOLPE²² to select the more informative parameters to define the best PLS model. Six parameters out of 29 were selected to be the more important (Sfit; DipMom; HOMO; MW; Volume and G_CDS_{aq}). The optimal number of principle components (PCs) was then chosen on the basis of the highest cross-validated q^2 value and the smallest standard deviation error of prediction (SDEP). Final PLS with

Table 1. PR enzyme assay and cytotoxicity of indole and pyrrole derivatives **1–2**

							
							
Compd	X	R ₁	R ₂	R ₃	R ₄	CC ₅₀ ^a	IC ₅₀ ^b
1a	—	H	COOEt	COOMe	—	39	nd
1b	—	H	CONH- <i>tert</i> -Bu	COOMe	—	39	114
1c	—	H	CONH- <i>tert</i> -Bu	CONH- <i>tert</i> -Bu	—	27	57
1d	—	Cl	COOEt	COOMe	—	39	72
1e	—	Cl	CONH- <i>tert</i> -Bu	COOMe	—	112	25
1f	—	Cl	CONH- <i>tert</i> -Bu	CONH- <i>tert</i> -Bu	—	66	nd
2a	NH	Ph	COOEt	H	2-Me	33	32% (200 μM)
2b	NH	Ph	COOEt	H	3-Me	22.2	29% (200 μM)
2c	NH	Ph	COOEt	H	4-Me	> 200	27% (200 μM)
2d	NH	Ph	COOEt	H	2-Cl	47.3	39% (200 μM)
2e	NH	Ph	COOEt	H	3-Cl	42.7	36% (200 μM)
2f	NH	Ph	COOEt	H	2-NH ₂	0.8	26% (200 μM)
2g	NH	Ph	COOEt	H	4-NH ₂	4.3	22% (200 μM)
2h	NH	Ph	COOEt	H	2-COOMe	37	174
2i	NH	Ph	CONH- <i>tert</i> -Bu	H	2-CONH- <i>tert</i> -Bu	101	161
2j	NH	Ph	COOEt	H	4-COOMe	61.3	118
2k	NH	Ph	COOEt	H	H	45	27% (200 μM)
2l	NH	Ph	COOEt	H	H	> 200	21% (200 μM)
2m	NH	Ph	H	COOMe	H	> 200	17% (200 μM)
2n	S	Ph	COOEt	H	H	75.3	24% (200 μM)
2o	S	Ph	COOEt	H	2-COOEt	50	200
2p	S	Ph	COOEt	H	2-CONH- <i>tert</i> -Bu	94	29% (200 μM)
2q	S	Ph	CONH- <i>tert</i> -Bu	H	2-CONH- <i>tert</i> -Bu	101	nd

nd, not determined.

^aCompound dose (μM) required to reduce the viability of mock-infected cells by 50% as determined by the MTT method.

^bCompound dose (μM) required to reduce by 50% the activity of PR enzyme.

no cross-validation was then carried out using the optimal number of PCs.

CoMFA-like studies (SYBYL-CoMFA,²³ GRID/GOLPE²²) are widely used tools for the study of QSARs at the 3-D level (3-D QSAR). Unlike the previous QSAR approach, that relies on calculated parameters, such a 3-D QSAR relate the biological activity of a series of molecules with molecular fields sampled at grid points of a large 3-D lattice box where the pre-aligned molecules are oriented. By means of suitable molecular probes positioned at each grid point, the 3-D QSAR columns are then computed using standard molecular mechanics fields, that is steric from Lennard-Jones interactions, electrostatic from Coulombic interactions. Partial least square (PLS) is usually the regression method to develop the relationship between the molecular fields and biological activity, where the optimum number of components (latent variables) is determined by the maximum q^2 value (cross-validated r^2). An important feature of this approach is the graphical representation indicating the regions where the variation of the molecular fields of different molecules in a data set is correlated with the variation of biological activity.

It is a well-established assumption to consider that a similar class of molecules (congeneric series) binds to the putative receptor site adopting a similar geometry and orientation. All test and training-set molecules were built using the MODIFY/ATOM module implemented in the program SYBYL²¹ using as template molecules the diarylbutanols AG1132, AG1157 and AG1284 to model respectively the *S* and *R* absolute configurations of the carbinol atoms.²⁴ A training set of 30 known diarylbutanol were compiled (Table 2) along with two test-sets of 20 molecules represented from the *S* and *R* configurations of the newly synthesized molecules of classes **1** and **2**.

Because of the high molecular similarity and employment of both ligand's absolute configurations in the training set and test set, no efforts were made to investigate different binding modes from those modeled from the crystal structures.

For the QSAR parameters and the CoMFA molecular alignment, all the modeled inhibitors were minimized inside HIV-PR by replacing the co-crystallized inhibitors in the complexes. Minimizations were performed using MACROMODEL 6.5²⁵ allowing an 8 Å core of atoms to relax during the minimization. An external fixed shell of 10 Å was also included for long-range interactions.

CoMFA calculations were performed with the QSAR module of SYBYL and the following parameters. The grid in which the aligned molecules were embedded was regularly spaced (2 Å) with dimensions of 28×24×20 Å. Steric and electrostatic interaction energies were calculated using a carbon sp³ probe with a +1 charge, a distance-dependent dielectric constant (1/ r), and an energetic cutoff of 30 kcal/mol with no electrostatic

interactions at sterically bad contacts. For both CoMFA fields, the atomic point charges were those included in the AMBER all-atom force field implemented in MacroModel 6.5. CoMFA regression analyses utilized the SYBYL implementation of the PLS algorithm, initially with leave-one-out (LOO) cross-validation to reduce the possibility of obtaining chance correlations and two principal components (PCs).

The optimal number of PCs was then chosen on the basis of the highest cross-validated q^2 value, the smallest standard error of prediction (SEP), and the minimum number of components. To improve the signal-to-noise ratio, the minimum sigma value was set to 2.0 kcal/mol. The steric and electrostatic field columns were weighted according to the CoMFA-STD default scaling option, where a field is considered as a whole and every CoMFA variable is affected by the overall field mean and standard deviation. Final PLS with no cross-validation was then carried out using the optimal number of PCs.

Results and Discussion

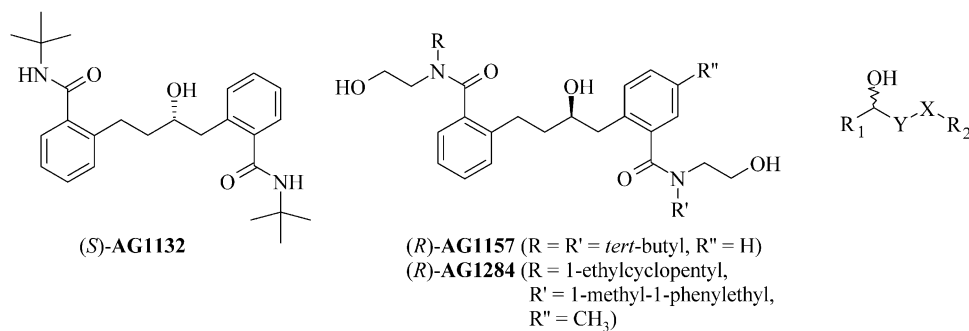
Anti-protease activity

Cytotoxicity and anti-protease activity of isopropanolamines **1–2** are reported in Table 1. As a rule indole derivatives **1** were more potent than their pyrrole counterparts (Table 1). Among the indole derivatives (**1a–f**), compounds **1b–1e** showed interesting PR inhibition with IC₅₀ ranging from 25 to 114 μM. The introduction of a chlorine atom at position 5 of the indole ring increased the activity (compare **1e** and **1b**). In the pyrrole series (**2a–q**), only compounds **2h–j** and **2o** showed some slight inhibitory activity in the PR enzyme assay.

Among tested compounds, *tert*-butyl derivatives (**1b, c, e** and **2i**) showed the highest anti-PR activity with IC₅₀ ranging from 25 to 161 μM, with the sole exception of the thio derivative **2p**. These data demonstrate the crucial role of *tert*-butylamide group to obtain derivatives with any anti-PR activity. Interesting potency was shown by esters **1d** and **2h** (IC₅₀=72 and 174 μM respectively) or mixed amidoester derivatives **1e** and **1b** (IC₅₀=25 and 114 μM). The slight activity of the *ortho*-ester **2h** (IC₅₀=174 μM) was retained when the ester group was shifted to the *para* position (**2j**, IC₅₀=118 μM), while replacement of carbomethoxy group with methyl, chlorine, methoxy or amino group led to inactive anti-PR compounds. The anti-PR activities were evaluated by Prof. Chi-Huey Wong, The Scripps Research Institute, La Jolla, CA, USA.²⁶

Finally, only a few compounds (viz., **2c, 2l**, and **2m**) were not cytotoxic for MT-4 cells at doses as high as 200 μM, whereas the majority of propanolamines derivatives showed CC₅₀ values at concentration ranging between 0.8 and 113.5 μM.

The most active derivatives in anti-protease assays, namely indoles **1**, were tested for their capability to

Table 2. Training set of diarylbutanols

Compd		pIC ₅₀	Conf.	R ₁	X-Y	R ₂	Name		Refs
AG 1	1	4.92	R		CH ₂ -CH ₂		ag1132R	PNAS 5R	14
AG 2	2	4.92	S		CH ₂ -CH ₂		ag1132R	PNAS 5R	14
AG 3	3	6.25	R		CH ₂ -CH ₂		ag1157R	PNAS 9S	14
AG 4	4	6.25	S		CH ₂ -CH ₂		ag1157S	PNAS 9S	14
AG 5	5	8.31	R		CH ₂ -CH ₂		ag1284R	PNAS 12R	14
AG 6	6	5.85	S		CH ₂ -CH ₂		ag1284S	PNAS 12S	14
AG 7	7	4.76	R		CH ₂ -CH ₂		JMC1996	15R	13
AG 8	8	4.76	S		CH ₂ -CH ₂		JMC1996	15S	13
AG 9	9	5.96	R		CH ₂ -CH ₂		JMC1996	16R	13

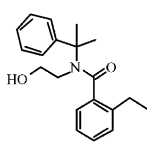
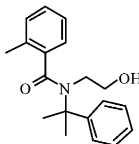
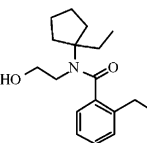
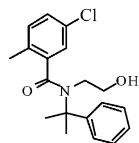
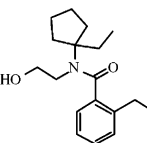
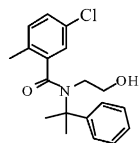
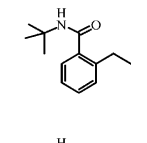
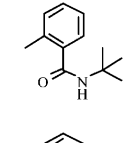
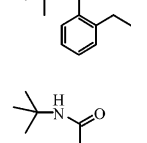
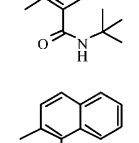
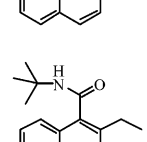
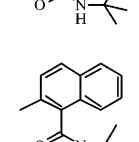
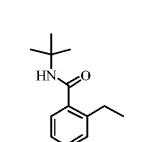
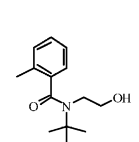
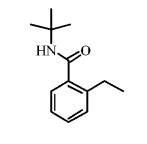
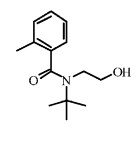
(continued on next page)

Table 2 (continued)

Compd		pIC ₅₀	Conf.	R ₁	X–Y	R ₂	Name		Refs
AG 10	10	5.96	<i>S</i>		CH ₂ –CH ₂		JMC1996	16 <i>S</i>	13
AG 11	11	6.22	<i>R</i>		CH ₂ –CH ₂		JMC1996	20 <i>R</i>	13
AG 12	12	6.22	<i>S</i>		CH ₂ –CH ₂		JMC1996	20 <i>S</i>	13
AG 13	13	5.46	<i>S</i>		CH ₂ –CH ₂		JMC1996	21 <i>S</i>	13
AG 14	14	5.46	<i>R</i>		CH ₂ –CH ₂		JMC1996	21 <i>R</i>	13
AG 15	15	4.90	<i>R</i>		CH ₂ –S		JMC1996	5 <i>R</i>	13
AG 16	16	4.90	<i>S</i>		CH ₂ –S		JMC1996	5 <i>S</i>	13
AG 17	17	4.22	<i>R</i>		CH ₂ –NH		JMC1996	7 <i>R</i>	13
AG 18	18	4.22	<i>S</i>		CH ₂ –NH		JMC1996	7 <i>S</i>	13
AG 19	19	7.35	<i>R</i>		CH ₂ –CH ₂		PNAS	10 <i>R</i>	14
AG 20	20	7.35	<i>S</i>		CH ₂ –CH ₂		PNAS	10 <i>R</i>	14
AG 21	21	7.96	<i>R</i>		CH ₂ –CH ₂		PNAS	11 <i>R</i>	14

(continued on next page)

Table 2 (continued)

Compd		pIC ₅₀	Conf.	R ₁	X–Y	R ₂	Name		Refs
AG 22	22	7.96	<i>S</i>		CH ₂ –CH ₂		PNAS	11 <i>S</i>	14
AG 23	23	9.00	<i>R</i>		CH ₂ –CH ₂		PNAS	13 <i>R</i>	14
AG 24	24	9.00	<i>S</i>		CH ₂ –CH ₂		PNAS	13 <i>S</i>	14
AG 25	25	4.37	<i>R</i>		CH ₂ –S		PNAS	4 <i>R</i>	14
AG 26	26	4.37	<i>S</i>		CH ₂ –S		PNAS	4 <i>S</i>	14
AG 27	27	4.60	<i>R</i>		CH ₂ –CH ₂		PNAS	7 <i>R</i>	14
AG 28	28	6.32	<i>S</i>		CH ₂ –CH ₂		PNAS	7 <i>S</i>	14
AG 29	29	4.76	<i>R</i>		CH ₂ –S		PNAS	8 <i>R</i>	14
AG 30	30	4.76	<i>S</i>		CH ₂ –S		PNAS	8 <i>S</i>	14

selectively inhibit the HIV-1-induced cytopathic effect in de novo infected MT-4 cells. Unfortunately, none of the compounds under investigation inhibited HIV-1 multiplication at concentrations below those cytotoxic for MT-4 cells (data not shown), probably due to a low cell penetration.

Molecular Modeling and QSAR

QSAR. The calculated parameters when correlated with the reported IC₅₀ of the training-set led to an internal self-consistent PLS model showing q^2 value of 0.751

with an associated SEP value of 0.743 using only 2 PCs. The non-cross-validated PLS resulted in a conventional correlation coefficient (r^2) value of 0.812 (Fig. 2) and a standard error of estimation (SEE) of 0.646 log unit of IC₅₀ (F test = 58.252). The resulting QSAR regression equation achieved a strong correlation between the calculated parameters and the biological activity. In general the more important parameters were the steric descriptors (*MW* and *Volume*) since their global contribution to the regression equation represent more than 66% of the total (Table 3). This agrees with the fact that the bigger are the structures, the better they can fit

inside HIV-PR active site with more interaction with the enzyme subsites.^{27,28}

$$\begin{aligned} \text{pIC}_{50} = & -4.284 - (0.659) * \text{Sfit} + (0.010) * \text{Dip-mom} \\ & - (0.340) * \text{HOMO} + (0.008) * \text{MW} \\ & + (0.008) * \text{Volume} - (0.053) * \text{G_CDS_aq} \end{aligned}$$

The QSAR model, when applied to the newly synthesized compound **1b–e** and **2a–p** (used as external test-set) calculated their pIC_{50} values (Table 4) with minimal errors of prediction (Average Absolute Error of Prediction for *R* configurations set, $\text{AAEP}_R = 0.36 \text{ pIC}_{50}$, Average Absolute Error of Prediction for *S* configurations set, $\text{AAEP}_S = 0.48 \text{ pIC}_{50}$). Moreover, the QSAR model successfully predicted as inactive, compounds **2a–g**, **2k–n**, with the sole exception of **2p** that was predicted an order of magnitude higher than the experimental value. Application of different arbitrary activity values to the inactive derivatives, such as 40 and 60% of the least active compound, led to minimal difference in the AAEPs values. ($\text{AAEP}_{R-40\%} = 0.33 \text{ pIC}_{50}$, $\text{AAEP}_{S-40\%} = 0.46 \text{ pIC}_{50}$, $\text{AAEP}_{R-60\%} = 0.41 \text{ pIC}_{50}$, $\text{AAEP}_{S-60\%} = 0.51 \text{ pIC}_{50}$).

CoMFA. In developing a CoMFA model, the alignment of the molecular training-set is a crucial part of the 3-D QSAR. Since structural information on the binding

mode for some of Agouron's compounds were available from crystalline complexes, molecular alignment was achieved by minimization of newly modeled HIV-PR/inhibitor complexes upon replacement of the co-crystallized compound with the analogous compounds.

Cross-validation led to a model with an optimal number of PC of 2, a q^2 value of 0.607 and a SEP of 0.933. The corresponding non-cross-validated analysis (2 PCs) resulted in a fitted r^2 value of 0.869 (Fig. 2), with a SEE of 0.540 (F-test = 89.169).

The CoMFA model is in a good agreement with the previous QSAR model showing a major contribution of the steric field (Table 5) over the electrostatic field. Moreover, the 3-D QSAR model was able to successfully predict the anti-PR active pIC_{50} (Table 4, $\text{AAEP}_R = 0.63 \text{ pIC}_{50}$, $\text{AAEP}_S = 0.74 \text{ pIC}_{50}$).

Beside the models' agreement, the 3-D QSAR correctly showed (Table 4) its inability to discriminate anti-PR active compounds (**1b–e**, **2h–j** and **2o**) from inactive compounds (**2a–g** and **2k–n**) since they were docked in the enzyme active site although they do not compete with any significant affinity. In the previous QSAR model, the explicative variable were mostly chemical and physical descriptors of ligands alone, and thus the final regression equation is totally independent from molecular alignment; while in the CoMFA model, the molecules are all embedded in a three-dimensional grid

Table 3. Relative contributions of the calculated parameters to the regression equation

Parameter	Description	Norm. Coeff.	Fraction
Sfit	Steric fit between ligand and receptor ¹⁸	0.087	0.074
Dip-Mom	Dipole moment (AMSOL ²⁹)	0.058	0.050
HOMO	HOMO ligand energy (AMSOL ²⁹)	0.126	0.108
MW	Molecular weight (AMSOL ²⁹)	0.391	0.334
Volume	Molecular volume (AMSOL ²⁹)	0.381	0.326
G_CDS_aq	Cavity-dispersion-solvent free energy (AMSOL ²⁹)	0.127	0.109

Table 4. Predictions of compounds **1b–e** and **2a–p**

Compd	Actual pIC_{50}	pIC_{50} QSAR predictions		pIC_{50} CoMFA predictions	
		<i>R</i> Configuration	<i>S</i> Configuration	<i>R</i> Configuration	<i>S</i> Configuration
1b	4.24	4.169	3.960	4.365	4.776
1c	4.54	4.865	4.756	4.593	5.192
1d	4.44	4.203	4.261	4.599	4.755
1e	4.90	4.498	4.478	4.459	4.486
2a	3.69	3.579	3.480	5.058	5.072
2b	3.69	3.34	3.385	5.099	5.132
2c	3.69	3.329	3.349	5.325	4.936
2d	3.69	3.654	3.913	5.277	4.466
2e	3.69	3.536	3.751	5.204	5.125
2f	3.69	3.273	3.508	5.082	4.879
2g	3.69	3.536	3.442	5.015	4.831
2h	4.06	4.005	4.240	4.908	4.834
2i	4.09	5.329	5.488	5.267	5.292
2j	4.23	4.316	4.309	5.149	4.971
2k	3.69	3.650	3.681	5.107	4.722
2l	3.69	3.183	2.180	5.029	4.833
2m	3.69	3.248	1.952	4.421	4.383
2n	3.69	3.145	3.047	4.964	5.160
2o	4.00	4.583	4.223	5.358	5.342
2p	3.69	4.817	4.794	5.316	5.570

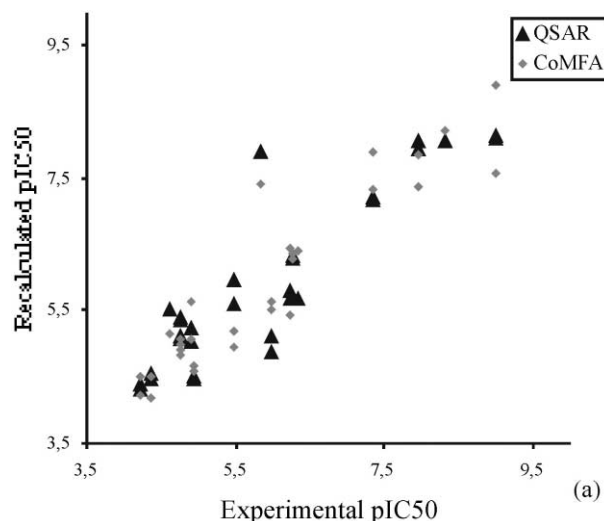


Figure 2. Training set experimental versus recalculated pIC_{50} .

Table 5. Relative contributions of CoMFA fields

Parameter	Norm. Coeff.	Fraction
COMFA (2145 vars) (Steric)	1.547	0.567
COMFA (2145 vars) (Electrostatic)	1.182	0.433

mimicking the receptor and assuming they all to bind to active site. The CoMFA analysis is thus totally dependent upon the molecular alignment.

Complementary to the previous QSAR model, the CoMFA model permits the graphical display of the results. The CoMFA steric and electrostatic field contour maps gave information about those regions where a modification of the chemical structure can enhance, or decrease, the biological activity. The surfaces are the representation of those lattice points, where differences in field values are correlated with differences in activity. In Fig. 3 are shown the maps for the CoMFA model ($StDEV \times COEFF$), where the orange contours represent regions of decreased tolerance for positive charge (20% contribution), the light blue contours represent regions of decreased tolerance for negative charge (80% contribution), the yellow contours represent regions of low steric tolerance (20% contribution) and the green contours represent regions of high steric tolerance (80% contribution).

The interpretation of these maps is highly subjective; the absence of lattice points does not mean that a given pharmacophoric element of the ligand has no influence on the biological activity, but only that almost all the compounds included in the training set exert similar steric and/or electrostatic influence in that particular area, or, alternatively, that the lack of polyhedra in some regions delineates a less explored space.

Table 6. Chemical and physical data of derivatives **1**, **2**, **5**, **6** and **11–14**

Compd	Formula	Mp ($^{\circ}C$)	Recrystn ^a Solvent	Yield	Chromat ^b System
1a	$C_{22}H_{24}N_2O_5$	97–99	a	47	A
1b	$C_{24}H_{29}N_3O_4$	oil	—	48	B
1c	$C_{27}H_{36}N_4O_3$	138–140	b	34	B
1d	$C_{22}H_{23}ClN_2O_5$	108–110	a	30	A
1e	$C_{24}H_{25}ClN_3O_4$	124–126	c	62	A
1f	$C_{27}H_{35}ClN_4O_3$	132–134	b	21	B
2a	$C_{23}H_{26}N_2O_3$	84–86	a	68	C
2b	$C_{23}H_{26}N_2O_3$	oil	—	65	C
2c	$C_{23}H_{26}N_2O_3$	130–132	c	76	C
2d	$C_{22}H_{23}ClN_2O_3$	oil	—	30	D
2e	$C_{22}H_{23}ClN_2O_3$	76–78	c	60	D
2f	$C_{23}H_{25}N_3O_3$	137–138	d	32	E
2g	$C_{22}H_{25}N_3O_3$	118–120	d	51	
2h	$C_{24}H_{26}N_2O_5$	oil	—	98	D
2i	$C_{29}H_{38}N_4O_3$	73–74	a	44	G
2j	$C_{24}H_{26}N_4O_5$	121–123	c	88	H
2k	$C_{22}H_{23}ClN_2O_3$	91–93	b	58	D
2l	$C_{16}H_{20}N_2O_3$	107–109	c	66	I
2m	$C_{16}H_{20}N_2O_3$	78–80	a	93	I
2n	$C_{22}H_{23}NO_3S$	oil	—	64	D
2o	$C_{25}H_{27}NO_5S$	oil	—	100	D
2p	$C_{27}H_{32}N_2O_4S$	oil	—	68	L
2q	$C_{29}H_{37}N_3O_3S$	96–98	c	34	H
6	$C_{14}H_{15}NO_3$	53–54	a	58	B
6	$C_{14}H_{14}ClNO_3$	83–84	a	30	D
11	$C_{16}H_{17}NO_3$	oil	—	42	D
12	$C_{16}H_{16}ClNO_3$	53–55	a	31	D
13	$C_{10}H_{13}NO_3$	oil	—	96	M
14	$C_{10}H_{13}NO_3$	oil	—	55	D

^aRecrystallization solvents. a: Cyclohexane; b: benzene; c: benzene/cyclohexane; d: ethanol.

^bChromatography eluent. A: *n*-hexane/ethyl ether 2:1; B: *n*-hexane/ethyl ether 1:1; C: ethyl acetate/chloroform 1:3; D: chloroform; E: ethyl acetate/chloroform 1:1; F: ethyl acetate; G: ethyl acetate/chloroform 1:5; H: ethyl acetate/chloroform 1:4; I: *n*-hexane/acetone 5:2; L: ethyl acetate/chloroform 1:2; M: ethyl acetate/chloroform 1:20.

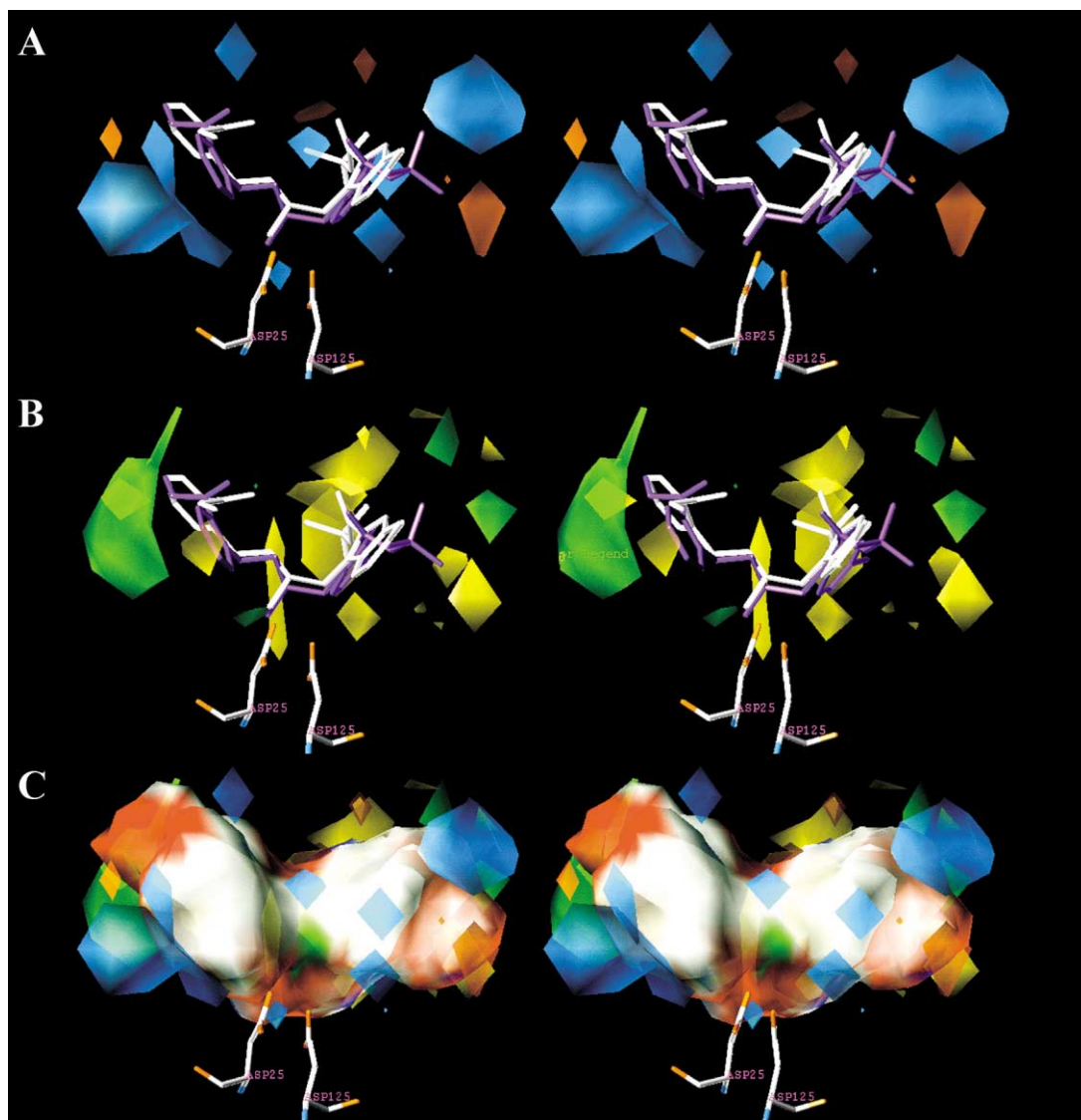


Figure 3. The contours of the electrostatic map are shown in orange and light blue (A), and those of the steric map are shown in yellow and green (B). Greater values of 'Bio-Activity Measurement' are correlated with: more bulk near green; less bulk near yellow; more positive charge near light blue, and more negative charge near orange. In C are showed the CoMFA contours overlapped to the HIV-Pr site color-coded by atom types. In A and B the two enantiomers of compound **2e** (*S* in white and *R* in purple) are also shown to help interpretation.

As can be seen in Fig. 3A, big light blue polyhedra are situated near the region where the more active compounds show a positive potential (i.e., an amidic or hydroxylic hydrogen) by which a hydrogen bond can take place, in fact, in ref 12 is reported on the experimental hydrogen-binding scheme of some Agouron's compound. The introduction of hydrogen-bonding groups, where lacking in this part of the inhibitors, could enhance the complex formation. On the other hand, little orange polyhedra are shown in those region where hydroxyethyl oxygen is present in the more potent compounds. Four yellow polyhedra (Fig. 3B) are situated that correspond to enzyme sub sites S1, S1', S2 and S2' meaning that it is not possible to enhance the bulkiness of the molecules in these regions, but instead for some molecules, the decrease of steric hindrance in this spatial region could relieve the ligand–receptor steric interaction leading to more active compounds. Two green polyhedra are instead shown to correspond to the S3 and S3' sub sites

that in some cases are partially filled by the ethyl portion of the hydroxyethyl group of the highly active compounds. In Figure 3C is shown the superposition of the CoMFA contour maps with the HIV-PR internal surface (atom type color coded) by which is possible to observe the good agreement between the red surface parts (amide oxygen of Gly27/127 and Asp30/130) with the CoMFA blue spots, and the white parts (enzyme backbone and hydrophobic side chains) with the CoMFA yellow polyhedra. The latter observation fully supports the use of a CoMFA model to describe the ligand–receptor interactions, of course, when molecular alignment is based on crystallographic information.

Conclusions

A series of *N*-aryl-pyrrolyl and *N*-aryl-indolyisopropanolamine derivatives were designed and synthesized as

inhibitors of HIV-1 PR (transition-state analogues). The cited compounds are strictly related to diarylbutanols^{12–14} synthesized by Agouron Pharmaceuticals and were tested against HIV-1 PR showing interesting activity for such simple molecules. In fact, a number of indolyl derivatives showed anti-PR activity with IC_{50} ranging from 25 to 114 μ M. Unfortunately, few pyrrolyl derivatives showed higher IC_{50} s (118–200 μ M) as most of them were unable to inhibit the PR activity at concentrations lower than 200 μ M. The ability of the most potent PR inhibitors (viz., compounds **1**) to block HIV-1 virus replication, was tested in cell-based assays, but no indolyl derivative showed effective concentrations (EC_{50}) for viral replication lower than the cytotoxic concentration.

QSAR and CoMFA models were developed using as the training set 30 of Agouron's HIV-1 PR inhibitors belonging to the diarylbutanols series. The models obtained were then used as tools to investigate on the binding mode of newly tested classes **1** and **2**. The agreement between the predicted and the experimental pIC_{50} values suggests that the new anti-PR active classes **1** and **2** likely bind into the enzyme active site similarly to the diarylbutanol series that were used as template for the molecular modeling and CoMFA alignment of the tested derivatives.

Experimental

Chemistry

Melting points were determined on a Büchi 530 melting point apparatus and are uncorrected. Infrared (IR) spectra (Nujol mulls) were recorded on a Perkin–Elmer 297 instrument. 1H NMR spectra were recorded at 200 MHz on a Bruker AC 200 spectrometer. Chemical shifts are reported in δ (ppm) units relative to the tetramethylsilane (TMS). All compounds were routinely checked by TLC and 1H NMR. TLC was performed by using Stratocrom SIF Fluka (silica gel precoated plates with fluorescent indicator) or Stratocrom ALF Fluka (aluminum oxide precoated plates with fluorescent indicator). Developed plates were visualized by UV light. Chromatographic purifications were performed on Merck aluminum oxide (70–230 mesh) and Merck silica gel (70–230 mesh). Solvents were reagent grade and, when necessary, were purified and dried by standard methods. Concentration of solutions after reactions and extractions involved the use of a rotary evaporator operating at a reduced pressure of approximately 20 torr. Organic solutions were dried over anhydrous sodium sulfate. Analytical results agreed to within $\pm 0.40\%$ of the theoretical values. Microanalyses were performed by Laboratories of Dipartimento di Scienze Farmaceutiche, Università di Padova, Italy. Chemical and physical data of newly synthesized compounds **1–2**, **5–6** and **11–14** are reported in Table 6.

Syntheses

Specific examples presented below illustrate general synthetic procedures.

Ethyl 1-oxiranylmethyl-4-phenyl-1H-pyrrole-3-carboxylate (11). A well stirred suspension of ethyl 4-phenyl-1H-pyrrole-3-carboxylate (10.0 g, 46.5 mmol), anhydrous potassium carbonate (12.8 g, 93 mmol) and epichlorohydrin (5.0 g, 54 mmol) in dry *N,N*-dimethylformamide (50 mL), was heated at 90 °C for 3 h. After cooling at room temperature, the mixture was treated with water (200 mL) and extracted with ethyl acetate (3 \times 100 mL). The collected organic extracts were washed with brine (3 \times 300 mL), dried and the solvent was evaporated to give crude derivative which was chromatographed on silica gel column (chloroform as eluent) to afford pure **11** (5.3 g, 42% yield): IR: ν 1700 (CO) cm^{-1} ; 1H NMR: δ 1.28 (t, 3H, $J_1 = 7.2$ Hz, CH_3), 2.57 (dd, 1H, $J_{gem} = 4.6$ Hz, $J_{vic1} = 2.5$ Hz, oxyrane CHH), 2.90 (dd, 1H, $J_{gem} = 4.6$ Hz, $J_{vic2} = 4.0$ Hz, oxyrane CHH), 3.30 (m, 1H, CH), 3.95 (m, 1H, CHH–pyrrole), 4.22 (m, 3H, CHH–pyrrole and CH_2CH_3), 6.75 (d, 1H, $J_2 = 2.5$ Hz, pyrrole C5-H), 7.30–7.50 (m, 6H, pyrrole C2-H and benzene H); anal. $C_{16}H_{17}NO_3$ (271.32) C, H, N.

This procedure was used for the synthesis of oxiranes **5**, **6** and **12–14** and their spectroscopic data are reported below

5. IR: ν 1695 (CO) cm^{-1} ; 1H NMR: δ 1.42 (t, 3H, $J = 7.2$ Hz, CH_3), 2.52 (dd, 1H, $J_{gem} = 4.4$ Hz, $J_{vic1} = 2.5$ Hz, oxyrane CHH), 2.77 (dd, 1H, $J_{gem} = 4.4$ Hz, $J_{vic2} = 4.4$ Hz, oxyrane CHH), 3.37 (m, 1H, CH), 4.36 (q, 2H, $J = 7.2$ Hz, CH_2CH_3), 4.55 (dd, 1H, $J_{gem} = 15.0$ Hz, $J_{vic3} = 5.1$ Hz, CHH-indole), 5.03 (dd, 1H, $J_{gem} = 15.0$ Hz, $J_{vic3} = 3.1$ Hz, CHH-indole), 7.12–7.69 (m, 5H, indole H); anal. $C_{14}H_{15}NO_3$ (245.28) C, H, N.

6. IR: ν 1700 (CO) cm^{-1} ; 1H NMR: δ 1.42 (t, 3H, $J = 7.2$ Hz, CH_3), 2.48 (dd, 1H, $J_{gem} = 4.4$ Hz, $J_{vic1} = 2.5$ Hz, oxyrane CHH), 2.79 (dd, 1H, $J_{gem} = 4.4$ Hz, $J_{vic2} = 4.4$ Hz, oxyrane CHH), 3.36 (m, 1H, CH), 4.33–4.52 (m, 3H, CHH-indole and CH_2CH_3), 5.07 (dd, 1H, $J_{gem} = 15.2$ Hz, $J_{vic3} = 2.8$ Hz, CHH-indole), 7.25–7.64 (m, 4H, indole H); anal. $C_{14}H_{14}ClNO_3$ (280.73) C, H, Cl, N.

12. IR: ν 1690 (CO) cm^{-1} ; 1H NMR: δ 1.25 (t, 3H, $J_1 = 7.2$ Hz, CH_3), 2.51 (dd, 1H, $J_{gem} = 4.5$ Hz, $J_{vic1} = 2.6$ Hz, oxyrane CHH), 2.86 (dd, 1H, $J_{gem} = 4.5$ Hz, $J_{vic2} = 4.5$ Hz, oxyrane CHH), 3.27 (m, 1H, CH), 3.87 (dd, 1H, $J_{gem} = 14.8$ Hz, $J_{vic3} = 6.0$ Hz, CHH–pyrrole), 4.15–4.26 (m, 3H, CHH–pyrrole and CH_2CH_3), 6.70 (d, 1H, $J_2 = 2.6$ Hz, pyrrole C5-H), 7.26–7.44 (m, 5H, pyrrole C2-H and benzene H); anal. $C_{16}H_{16}ClNO_3$ (305.76) C, H, Cl, N.

13. IR: ν 1700 (CO) cm^{-1} ; 1H NMR: δ 1.35 (t, 3H, $J = 7.0$ Hz, CH_3), 2.48 (dd, 1H, $J_{gem} = 4.7$ Hz, $J_{vic1} = 2.5$ Hz, oxyrane CHH), 2.85 (dd, 1H, $J_{gem} = 4.7$ Hz, $J_{vic2} = 4.5$ Hz, oxyrane CHH), 3.26 (m, 1H, CH), 3.93 (dd, 1H, $J_{gem} = 14.8$ Hz, $J_{vic3} = 5.7$ Hz, CHH–pyrrole), 4.18–4.34 (m, 3H, CHH–pyrrole and CH_2CH_3), 6.60–6.68 (m, 2H, pyrrole C4-H and C5-H), 7.35 (dd, 1H, $J_{2,4} = 1.5$ Hz, $J_{2,5} = 1.7$ Hz, pyrrole C2-H); anal. $C_{10}H_{13}NO_3$ (195.22) C, H, N.

14. IR: ν 1680 (CO) cm^{-1} ; ^1H NMR: δ 1.39 (t, 3H, $J=7.0$ Hz, CH_3), 2.47 (dd, 1H, $J_{\text{gem}}=4.7$ Hz, $J_{\text{vic1}}=2.5$ Hz, oxyrane CHH), 2.83 (dd, 1H, $J_{\text{gem}}=4.7$ Hz, $J_{\text{vic2}}=4.5$ Hz, oxyrane CHH), 3.40 (m, 1H, CH), 4.25–4.37 (m, 3H, CHH -pyrrole and CH_2CH_3), 4.83 (dd, 1H, $J_{\text{gem}}=14.7$ Hz, $J_{\text{vic3}}=5.6$ Hz, CHH -pyrrole), 6.19 (dd, 1H, $J_{3,4}=4.0$ Hz, $J_{4,5}=2.6$ Hz, pyrrole C4-H), 6.92–7.03 (m, 2H, pyrrole C3-H and C5-H); anal. $\text{C}_{10}\text{H}_{13}\text{NO}_3$ (195.22) C, H, N.

Ethyl 1-[3-(2-methyl)phenylamino-2-hydroxypropyl]-4-phenyl-1H-pyrrole-3-carboxylate (2a). A mixture of **11** (500 mg, 1.9 mmol) and 2-methylaniline (200 mg, 1.9 mmol) were heated at 90°C for 5 h. The cooled mixture was dissolved in chloroform and chromatographed on silica gel column (chloroform as eluent) to obtain pure **2a** (490 mg, 68% yield): IR: ν 3400 (NH and OH), 1680 (CO) cm^{-1} ; ^1H NMR: δ 1.26 (t, 3H, $J=7.0$ Hz, CH_2CH_3), 2.16 (s, 3H, CH_3), 2.55 (bs, 1H, OH), 3.16 (dd, 1H, $J_{\text{gem}}=13.0$ Hz, $J_{\text{vic1}}=7.3$ Hz, CHHNNH), 3.33 (dd, 1H, $J_{\text{gem}}=13.0$ Hz, $J_{\text{vic2}}=3.9$ Hz, CHHNNH), 3.80–4.25 (m, 6H, CH_2 -pyrrole, CH_2CH_3 , CH and NH), 6.58–7.50 (m, 11H, pyrrole and benzene H); anal. $\text{C}_{23}\text{H}_{26}\text{N}_2\text{O}_3$ (378.47) C, H, N.

The cited reaction was used to obtain propanolamines **1a**, **1d**, **2b–h**, **2j–m**, while arylthiopropans **2n–o** were obtained with the same procedure using ethanol as a solvent and refluxing the mixture for 6 h. Spectroscopic data of these derivatives are reported below:

1a. IR: ν 3480, 3340 (NH and OH), 1680 (CO) cm^{-1} ; ^1H NMR: δ 1.40 (t, 3H, $J_1=7.2$ Hz, CH_2CH_3), 3.07 (d, 1H, $J_2=4.2$ Hz, OH), 3.37 (m, 2H, CH_2NH), 3.85 (s, 3H, OCH_3), 4.31–4.41 (m, 3H, CH_2CH_3 and CH), 4.67 (m, 2H, CH_2 -indole), 6.56–7.93 (m, 12H, indole and benzene H), 8.03 (bs, 1H, NH); anal. $\text{C}_{22}\text{H}_{24}\text{N}_2\text{O}_5$ (396.44) C, H, N.

1d. IR: ν 3490, 3340 (NH and OH), 1680 (CO) cm^{-1} ; ^1H NMR: δ 1.40 (t, 3H, $J=7.0$ Hz, CH_2CH_3), 2.95 (bs, 1H, OH), 3.36 (m, 2H, CH_2NH), 3.85 (s, 3H, OCH_3), 4.32–4.42 (m, 3H, CH_2CH_3 and CH), 4.70 (m, 2H, CH_2 -indole), 6.59–6.71 (m, 2H, anthranilate C3-H and C5-H), 7.21–7.93 (m, 6H, indole and benzene H), 8.03 (bs, 1H, NH); anal. $\text{C}_{22}\text{H}_{23}\text{ClN}_2\text{O}_3$ (430.89) C, H, Cl, N.

2b. IR: ν 3380 (NH and OH), 1680 (CO) cm^{-1} ; ^1H NMR: δ 1.22 (t, 3H, $J=7.0$ Hz, CH_2CH_3), 2.27 (s, 3H, CH_3), 2.80 (bs, 1H, OH), 3.05 (dd, 1H, $J_{\text{gem}}=13.0$ Hz, $J_{\text{vic1}}=7.2$ Hz, CHHNNH), 3.24 (dd, 1H, $J_{\text{gem}}=13.0$ Hz, $J_{\text{vic2}}=3.8$ Hz, CHHNNH), 3.83–4.23 (m, 6H, CH_2 -pyrrole, CH_2CH_3 , CH and NH), 6.41–7.49 (m, 11H, pyrrole and benzene H); anal. $\text{C}_{23}\text{H}_{26}\text{N}_2\text{O}_3$ (378.47) C, H, N.

2c. IR: ν 3440, 3380 (NH and OH), 1670 (CO) cm^{-1} ; ^1H NMR: δ 1.22 (t, 3H, $J=7.2$ Hz, CH_2CH_3), 2.24 (s, 3H, CH_3), 2.60 (bs, 1H, OH), 3.05 (dd, 1H, $J_{\text{gem}}=13.0$ Hz, $J_{\text{vic1}}=7.4$ Hz, CHHNNH), 3.25 (dd, 1H, $J_{\text{gem}}=13.0$ Hz, $J_{\text{vic2}}=3.7$ Hz, CHHNNH), 3.70–4.24 (m, 6H, CH_2 -pyrrole, CH_2CH_3 , CH and NH), 6.49–7.77 (m, 11H, pyrrole and benzene H); anal. $\text{C}_{23}\text{H}_{26}\text{N}_2\text{O}_3$ (378.47) C, H, N.

2d. IR: ν 3400 (NH and OH), 1680 (CO) cm^{-1} ; ^1H NMR: δ 1.23 (t, 3H, $J=7.1$ Hz, CH_3), 2.65 (bs, 1H, OH), 3.08–3.35 (m, 2H, CH_2NH), 3.90–4.24 (m, 5H, CH_2 -pyrrole, CH_2CH_3 , and CH), 4.60 (bs, 1H, NH), 6.62–7.49 (m, 11H, pyrrole and benzene H); anal. $\text{C}_{22}\text{H}_{22}\text{ClN}_2\text{O}_3$ (398.89) C, H, Cl, N.

2e. IR: ν 3380 (NH and OH), 1670 (CO) cm^{-1} ; ^1H NMR: δ 1.23 (t, 3H, $J=7.1$ Hz, CH_3), 2.66 (bs, 1H, OH), 3.05 (dd, 1H, $J_{\text{gem}}=12.8$ Hz, $J_{\text{vic1}}=7.1$ Hz, CHHNNH), 3.23 (dd, 1H, $J_{\text{gem}}=12.8$ Hz, $J_{\text{vic2}}=3.7$ Hz, CHHNNH), 3.88–4.24 (m, 6H, CH_2 -pyrrole, CH_2CH_3 , CH and NH), 6.45–7.48 (m, 11H, pyrrole and benzene H); anal. $\text{C}_{22}\text{H}_{22}\text{ClN}_2\text{O}_3$ (398.89) C, H, Cl, N.

2f. IR: ν 3400, 3370, 3220, 3100 (NH_2 , NH and OH), 1670 (CO) cm^{-1} ; ^1H NMR: δ 1.23 (t, 3H, $J=7.1$ Hz, CH_3), 3.06 (dd, 1H, $J_{\text{gem}}=12.8$ Hz, $J_{\text{vic1}}=7.6$ Hz, CHHNNH), 3.26 (dd, 1H, $J_{\text{gem}}=12.8$ Hz, $J_{\text{vic2}}=3.7$ Hz, CHHNNH), 3.35 (bs, 4H, NH_2 , NH and OH), 3.90–4.25 (m, 5H, CH_2 -pyrrole, CH_2CH_3 , and CH), 6.61–6.86 (m, 5H, pyrrole C5-H and aniline H), 7.26–7.50 (m, 6H, pyrrole C2-H and benzene H); anal. $\text{C}_{22}\text{H}_{25}\text{N}_3\text{O}_3$ (379.46) C, H, N.

2g. IR: ν 3400, 3340, 3100 (NH_2 , NH and OH), 1670 (CO) cm^{-1} ; ^1H NMR: δ 1.23 (t, 3H, $J=7.1$ Hz, CH_3), 2.98 (dd, 1H, $J_{\text{gem}}=12.6$ Hz, $J_{\text{vic1}}=7.2$ Hz, CHHNNH), 3.19 (dd, 1H, $J_{\text{gem}}=12.6$ Hz, $J_{\text{vic2}}=3.5$ Hz, CHHNNH), 3.20 (bs, 4H, NH_2 , NH and OH), 3.85–4.25 (m, 5H, CH_2 -pyrrole, CH_2CH_3 , and CH), 6.55 (m, 4H, aniline H), 6.69 (d, 1H, $J_{2,5}=2.3$ Hz, pyrrole C5-H), 7.21–7.50 (m, 6H, pyrrole C2-H and benzene H); anal. $\text{C}_{22}\text{H}_{25}\text{N}_3\text{O}_3$ (379.46) C, H, N.

2h. IR: ν 3420, 3350 (NH and OH), 1670 (CO) cm^{-1} ; ^1H NMR: δ 1.23 (t, 3H, $J=7.1$ Hz, CH_2CH_3), 1.60 and 2.39 (2bs, 2H, NH and OH), 3.31 (m, 2H, CH_2NH), 3.86 (s, 3H, OCH_3), 4.02 (m, 2H, CH_2 -pyrrole), 4.14–4.24 (m, 3H, CH_2CH_3 and CH), 6.62–6.72 (m, 3H, pyrrole C5-H and anthranilate C3-H and C5-H), 7.21–7.50 (m, 7H, pyrrole C2-H, anthranilate C4-H and benzene H), 7.93 (m, 1H, anthranilate C6-H); anal. $\text{C}_{24}\text{H}_{26}\text{N}_2\text{O}_5$ (422.48) C, H, N.

2j. IR: ν 3380 (NH and OH), 1685 (CO) cm^{-1} ; ^1H NMR: δ 1.22 (t, 3H, $J_1=7.2$ Hz, CH_2CH_3), 2.79 (d, 1H, $J_2=4.2$ Hz, OH), 3.14–3.31 (m, 2H, CH_2NH), 3.85 (s, 3H, OCH_3), 3.90–4.10 (m, 3H, CH_2 -pyrrole and CH), 4.18 (q, 2H, $J_1=7.2$ Hz, CH_2CH_3), 4.50 (bs, 1H, NH), 6.56 (m, 2H, aniline C2-H and C6-H), 6.69 (d, 1H, $J_{2,5}=2.5$ Hz, pyrrole C5-H), 7.25–7.48 (m, 6H, pyrrole C2-H and benzene H), 7.85 (m, 2H, aniline C3-H and C5-H); anal. $\text{C}_{24}\text{H}_{26}\text{N}_2\text{O}_5$ (422.48) C, H, N.

2k. IR: ν 3280 (NH and OH), 1665 (CO) cm^{-1} ; ^1H NMR: δ 1.29 (t, 3H, $J=7.0$ Hz, CH_3), 2.50 (bs, 1H, OH), 3.20 (dd, 1H, $J_{\text{gem}}=13.2$ Hz, $J_{\text{vic1}}=7.2$ Hz, CHHNNH), 3.31 (dd, 1H, $J_{\text{gem}}=13.2$ Hz, $J_{\text{vic2}}=4.0$ Hz, CHHNNH), 3.95–4.29 (m, 6H, CH_2 -pyrrole, CH_2CH_3 , CH and NH), 6.66–7.47 (m, 11H, pyrrole and benzene H); anal. $\text{C}_{22}\text{H}_{23}\text{ClN}_2\text{O}_3$ (398.89) C, H, Cl, N.

2l. IR: ν 3480, 3440, 3340 (NH and OH), 1670 (CO) cm^{-1} ; ^1H NMR: δ 1.33 (t, 3H, $J_1=7.1$ Hz, CH_3), 2.50 (d, 1H, $J_2=3.6$ Hz, OH), 3.06 (dd, 1H, $J_{\text{gem}}=13.1$ Hz, $J_{\text{vic1}}=7.2$ Hz, CHHNH), 3.27 (dd, 1H, $J_{\text{gem}}=13.1$ Hz, $J_{\text{vic2}}=3.4$ Hz, CHHNH), 3.87–4.31 (m, 6H, CH_2 -pyrrole, CH_2CH_3 , CH and NH), 6.59–7.35 (m, 8H, pyrrole H and benzene H); anal. $\text{C}_{16}\text{H}_{20}\text{N}_2\text{O}_3$ (288.34) C, H, N.

2m. IR: ν 3380 (NH and OH), 1685 (CO) cm^{-1} ; ^1H NMR: δ 1.35 (t, 3H, $J=7.2$ Hz, CH_3), 2.96 (bs, 1H, OH), 3.08 (dd, 1H, $J_{\text{gem1}}=12.7$ Hz, $J_{\text{vic1}}=6.8$ Hz, CHHNH), 3.29 (dd, 1H, $J_{\text{gem1}}=12.7$ Hz, $J_{\text{vic2}}=4.2$ Hz, CHHNH), 4.10–4.34 (m, 5H, CHH-pyrrole, CH_2CH_3 , CH and NH), 4.60 (dd, 1H, $J_{\text{gem2}}=13.6$ Hz, $J_{\text{vic3}}=3.5$ Hz, CHH-pyrrole), 6.15 (dd, 1H, $J_{3,4}=4.0$ Hz, $J_{4,5}=2.7$ Hz, pyrrole C4-H), 6.63–7.25 (m, 7H, pyrrole C3-H and C5-H and benzene H); anal. $\text{C}_{16}\text{H}_{20}\text{N}_2\text{O}_3$ (288.34) C, H, N.

2n. IR: ν 3420 (OH), 1680 (CO) cm^{-1} ; ^1H NMR: δ 1.23 (t, 3H, $J_1=7.2$ Hz, CH_3), 2.71 (d, 1H, $J_2=3.2$ Hz, OH), 2.86 (dd, 1H, $J_{\text{gem}}=13.7$ Hz, $J_{\text{vic1}}=6.9$ Hz, CHHS), 3.03 (dd, 1H, $J_{\text{gem}}=13.7$ Hz, $J_{\text{vic2}}=4.5$ Hz, CHHS), 3.91–4.24 (m, 5H, CH_2 -pyrrole, CH_2CH_3 , and CH), 6.66 (d, 1H, $J_{2,5}=2.5$ Hz, pyrrole C5-H), 7.23–7.48 (m, 11H, pyrrole C2-H and benzene H); anal. $\text{C}_{22}\text{H}_{23}\text{NO}_3\text{S}$ (381.49) C, H, N, S.

2o. IR: ν 3440 (OH), 1700 (CO) cm^{-1} ; ^1H NMR: δ 1.23 (t, 3H, $J_1=7.1$ Hz, CH_2CH_3 pyrrole ester), 1.40 (t, 3H, $J_2=7.1$ Hz, CH_2CH_3 benzene ester), 2.86–3.13 (m, 2H, CH_2S), 3.27 (bs, 1H, OH), 4.04 (m, 3H, CH_2 -pyrrole and CH), 4.20 (q, 2H, $J_1=7.1$ Hz, CH_2CH_3 pyrrole ester), 4.37 (q, 2H, $J_2=7.1$ Hz, CH_2CH_3 benzene ester), 6.70 (d, 1H, $J_{2,5}=2.4$ Hz, pyrrole C5-H), 7.21–7.48 (m, 9H, pyrrole C2-H and benzene H), 7.88 (dd, 1H, $J_o=7.7$ Hz, $J_m=1.2$ Hz, phenylthio C3-H); anal. $\text{C}_{25}\text{H}_{27}\text{NO}_5\text{S}$ (453.55) C, H, N, S.

N-tert-Butyl 1-{2-hydroxy-3-[2-(tert-butylaminocarbonyl)phenylaminopropyl]-4-phenyl-1H-pyrrole-3-carboxamide (2i). *tert*-Butylamine (670 mg, 9.2 mmol) was added into a cooled solution ($T=-12^\circ\text{C}$) of trimethylaluminum (4.7 mL 2.0 M in hexane, 9.6 mmol) in toluene (45 mL) and the mixture was stirred at room temperature for 45 min, then cooled at 0°C and finally treated with a solution of **2h** (880 mg, 2.1 mmol) in toluene (30 mL). The resulting solution was refluxed for 12 h, then cooled at room temperature and treated with 1 N hydrochloric acid (100 mL) and finally extracted with ethyl acetate (3×50 mL). The organic extracts were collected, washed with brine (20 mL) and dried. Removal of the solvent gave a residue which was chromatographed on silica gel column (chloroform/ethyl acetate 2:1 as eluent then ethyl acetate and finally ethyl acetate/ethanol 1:1) to obtain 450 mg of **2i** (44% yield): IR: ν 3400, 3280 (NH and OH), 1620 (CO) cm^{-1} ; ^1H NMR: δ 1.18 (s, 9H, CCH_3 pyrrole), 1.44 (s, 9H, CCH_3 benzene), 3.32 (m, 2H, CH_2NH), 3.99–4.03 (m, 3H, CH_2 -pyrrole, and CH), 5.37 and 5.93 (2bs, 4H, CONH and OH), 6.61–6.71 (m, 3H, pyrrole C5-H and anthranilamide C3-H and C5-H), 7.24–7.38 (m, 8H, pyrrole C2-H, anthranilamide C4-H and C6-H and benzene H); anal. $\text{C}_{29}\text{H}_{38}\text{N}_4\text{O}_3$ (490.64) C, H, N.

With the same procedure were synthesized the amides **1b**, **c**, **1e**, **f**, **2p**, **q** and their spectroscopic data are reported below.

1b. IR: ν 3320, 3240 (NH and OH), 1680 (ester CO), 1630 (amide CO) cm^{-1} ; ^1H NMR: δ 1.48 (s, 9H, CCH_3), 3.41 (m, 2H, CH_2NH), 3.92 (s, 3H, OCH_3), 4.32 (m, 1H, CH), 4.61 (m, 2H, CH_2 -indole), 5.69 (bs, 1H, OH), 6.16 (bs, 1H, CONH), 6.58–7.40 (m, 7H, indole and benzene H), 8.10 (bs, 1H, NH aniline); anal. $\text{C}_{24}\text{H}_{29}\text{N}_3\text{O}_4$ (423.51) C, H, N.

1c. IR: ν 3360, 3260, 3160 (NH and OH), 1640 (amide CO) cm^{-1} ; ^1H NMR: δ 1.47 (s, 18H, CCH_3), 3.30–3.49 (m, 2H, CH_2NH), 4.27 (m, 1H, CH), 4.59 (m, 2H, CH_2 -indole), 5.67 (d, 1H, $J=4.4$ Hz, OH), 5.94 and 6.18 (2bs, 2H, CONH), 6.58–7.67 (m, 9H, indole and benzene H), 7.70 (bs, 1H, NH aniline); anal. $\text{C}_{27}\text{H}_{36}\text{N}_4\text{O}_3$ (464.61) C, H, N.

1e. IR: ν 3320, 3240, 3060 (NH and OH), 1680 (ester CO), 1625 (amide CO) cm^{-1} ; ^1H NMR: δ 1.47 (s, 9H, CCH_3), 3.39 (m, 2H, CH_2NH), 3.87 (s, 3H, OCH_3), 4.25 (m, 1H, CH), 4.55 (m, 2H, CH_2 -indole), 5.53 (d, 1H, $J=4.4$ Hz, OH), 6.19 (bs, 1H, CONH), 6.59–7.95 (m, 8H, indole and benzene H), 8.05 (bs, 1H, NH aniline); anal. $\text{C}_{24}\text{H}_{28}\text{ClN}_3\text{O}_4$ (457.96) C, H, Cl, N.

1f. IR: ν 3380, 3270, 3150 (NH and OH), 1640 (amide CO) cm^{-1} ; ^1H NMR: δ 1.47 (s, 18H, CCH_3), 3.22–3.53 (m, 2H, CH_2NH), 4.24 (m, 1H, CH), 4.58 (m, 2H, CH_2 -indole), 5.52 (bs, 1H, OH), 5.94 and 6.20 (2bs, 2H, CONH), 6.55–7.66 (m, 8H, indole and benzene H), 7.65 (bs, 1H, NH aniline); anal. $\text{C}_{27}\text{H}_{35}\text{ClN}_4\text{O}_3$ (499.05) C, H, Cl, N.

2p. IR: ν 3300 (NH and OH), 1700 (ester CO), 1630 (amide CO) cm^{-1} ; ^1H NMR: δ 1.23 (t, 3H, $J_1=7.1$ Hz, CH_2CH_3), 1.487 (s, 9H, CCH_3), 2.69 (dd, 1H, $J_{\text{gem}}=14.0$ Hz, $J_{\text{vic1}}=8.2$ Hz, CH_2S), 3.01 (dd, 1H, $J_{\text{gem}}=14.0$ Hz, $J_{\text{vic2}}=3.0$ Hz, CH_2S), 3.94–3.96 (m, 3H, CH_2 -pyrrole and CH), 4.17 (q, 2H, $J_1=7.1$ Hz, CH_2CH_3), 5.23 (d, 1H, $J_2=4.9$ Hz, OH), 5.78 (bs, 1H, CONH), 6.65 (d, 1H, $J_{2,5}=2.3$ Hz, pyrrole C5-H), 7.23–7.52 (m, 10H, pyrrole C2-H and benzene H); anal. $\text{C}_{27}\text{H}_{32}\text{N}_2\text{O}_4\text{S}$ (480.62) C, H, N, S.

2q. IR: ν 3400, 3260 (NH and OH), 1625 (CO) cm^{-1} ; ^1H NMR: δ 1.18 (s, 9H, CCH_3 pyrrole), 1.48 (s, 9H, CCH_3 benzene), 2.77 (dd, 1H, $J_{\text{gem}}=13.6$ Hz, $J_{\text{vic1}}=7.9$ Hz, CH_2S), 2.98 (dd, 1H, $J_{\text{gem}}=13.6$ Hz, $J_{\text{vic2}}=2.8$ Hz, CH_2S), 3.87–3.98 (m, 3H, CH_2 -pyrrole, and CH), 5.21 (d, 1H, $J=4.5$ Hz, OH), 5.34 (bs, 1H, CONH pyrrole), 5.88 (bs, 1H, CONH phenylthio), 6.60 (d, 1H, $J_{2,5}=2.3$ Hz, pyrrole C5-H), 7.22–7.38 (m, 10H, pyrrole C2-H and benzene H); anal. $\text{C}_{29}\text{H}_{37}\text{N}_3\text{O}_3\text{S}$ (507.69) C, H, N, S.

Microbiology

Compounds. Test compounds were dissolved in DMSO at an initial concentration of 200 mM and then were serially diluted in culture medium.

Cells. MT-4 cells [grown in RPMI 1640 containing 10% foetal calf serum (FCS), 100 UI/mL penicillin G and 100 $\mu\text{g}/\text{mL}$ streptomycin] were used for cytotoxicity and

anti-HIV-1 assays. Cell cultures were checked periodically for the absence of mycoplasma contamination with a MycoTect Kit (Gibco).

Cytotoxicity and anti-HIV assays. Activity against the HIV-1 (HIV-1, III_B strain, obtained from supernatants of persistently infected H9/III_B cells.) multiplication in acutely infected cells was based on inhibition of virus-induced cytopathogenicity in MT-4 cells. Briefly, 50 μ L of RPMI 10% FCS containing 1×10^4 cells were added to each well of flat-bottomed microtiter trays containing 50 μ L of medium and serial dilutions of test compounds. 20 μ L of an HIV-1 suspension containing 100 CCID₅₀ were then added. After a 4 day incubation at 37°C, the number of viable cells was determined by the 3-(4,5-dimethylthiazol-2-yl)-2,5-diphenyl-tetrazolium bromide (MTT) method. Cytotoxicity of compounds, based on the viability of mock-infected cells as monitored by the MTT method, was evaluated in parallel with their antiviral activity.

Acknowledgements

Thanks are due to Ministero della Sanità, Istituto Superiore di Sanità, Progetto AIDS 1999 (grant no. 40C.8) and to Italian MURST for partial support. Thanks are due to Professor Chi-Huey Wong, The Scripps Research Institute, La Jolla, CA, USA, for the PR enzyme assays.

Appendix A. Analytical results of newly synthesized derivatives 1a–f, 2a–e

Compd	Elemental analyses calculated/found				
	C	H	N	S	Cl
1a	66.65	6.10	7.07	—	—
	66.51	6.21	7.17	—	—
1b	68.07	6.90	9.92	—	—
	68.18	6.85	9.87	—	—
1c	69.80	7.81	12.06	—	—
	69.85	7.95	12.18	—	—
1d	61.32	5.38	6.50	—	8.23
	61.28	5.29	6.66	—	8.35
1e	62.95	6.16	9.18	—	7.74
	62.81	6.25	9.31	—	7.85
1f	64.98	7.07	11.23	—	7.10
	64.85	7.21	11.35	—	7.15
2a	72.99	6.92	7.40	—	—
	73.03	6.90	7.37	—	—
2b	72.99	6.92	7.45	—	—
	72.87	6.95	7.43	—	—
2c	72.99	6.92	7.40	8.65	—
	72.85	6.91	7.40	8.71	—
2d	66.24	5.81	7.02	7.99	8.89
	66.35	5.80	6.99	8.02	8.93
2e	66.24	5.81	7.02	9.76	8.89
	66.34	5.90	7.00	9.84	8.91

Appendix B. Analytical results of newly synthesized derivatives 2f–d

Compd	Elemental analyses calculated/found				
	C	H	N	S	Cl
2f	69.64	6.64	11.07	—	—
	69.60	6.67	11.03	—	—
2g	69.64	6.64	11.07	—	—
	69.60	6.58	11.05	—	—
2h	68.23	6.20	6.63	—	—
	68.18	6.31	6.43	—	—
2i	70.99	7.81	11.42	—	—
	71.03	7.73	11.64	—	—
2j	68.23	6.20	6.63	—	—
	68.21	6.15	6.58	—	—
2k	66.24	5.81	7.02	8.65	8.89
	66.14	5.87	7.12	8.71	8.91
2l	66.65	6.99	9.72	7.99	—
	66.71	7.00	9.51	8.02	—
2m	66.65	6.99	9.72	9.76	—
	66.63	6.88	9.83	9.84	—
2n	69.27	6.08	3.67	8.40	—
	69.21	6.07	3.69	8.41	—
2o	66.21	6.00	3.09	7.07	—
	66.01	6.18	3.10	7.05	—
2p	67.47	6.71	5.83	6.67	—
	67.23	6.73	5.91	6.71	—
2q	68.61	7.35	8.28	6.31	—
	68.51	7.09	8.48	6.41	—

Appendix C. Analytical results of newly synthesized derivatives 5, 6 and 11–14

Compd	Elemental analyses calculated/found				
	C	H	N	S	Cl
5	68.56	6.16	5.71	—	—
	68.51	6.13	5.83	—	—
6	59.90	5.39	4.99	—	12.63
	59.97	5.31	4.87	—	12.51
11	70.83	6.32	5.16	—	—
	70.81	6.40	5.25	—	—
12	62.85	5.27	4.58	—	11.60
	62.83	5.33	4.72	—	11.51
13	61.53	6.71	7.17	—	—
	61.50	6.68	7.15	—	—
14	61.53	6.71	7.17	—	—
	61.50	6.81	7.20	—	—

References and Notes

- Artico, M. *Farmaco* **1996**, *51*, 305.
- Martin, J. A.; Redshaw, S.; Thomas, G. J. *Prog. Med. Chem.* **1995**, *32*, 239.
- Appelt, K. *Perspect. Drug Discov. Des.* **1993**, *1*, 23.
- Roberts, N.; Martin, J.; Kinchington, D.; Broadhurst, A.; Craig, J.; Duncan, I.; Galpin, S.; Handa, B.; Kay, J.; Krohn, A.; Lambert, R.; Merrett, J.; Mills, J.; Parkes, K.; Redshaw, A.

- S.; Ritchie, A.; Taylor, D.; Thomas, G.; Machin, P. *Science* **1990**, 248, 358.
5. Kempf, D. J.; Marsh, K. C.; Denissen, J. F.; McDonald, E.; Vasavanonda, S.; Flentge, C. A.; Green, B. E.; Fino, L.; Park, C. H.; Kong, X. P.; Wideburg, N. E.; Saldivar, A.; Ruitz, L.; Kati, W. M.; Sham, H. L.; Robins, T.; Stewart, K. D.; Hsu, A.; Plattner, J. J.; Leonard, J. M.; Norbeck, D. W. *Proc. Natl. Acad. Sci. U.S.A.* **1995**, 92, 2484.
6. Dorsey, B. D.; Levin, R. B.; McDaniel, S. L.; Vacca, J. P.; Guare, J. P.; Darke, P. L.; Zugay, J. A.; Emini, E. A.; Schleif, W. A.; Quintero, J. C.; Lin, J. H.; Chen, I.-W.; Holloway, M. K.; Fitzgerald, P. M. D.; Axel, M. G.; Ostovic, D.; Anderson, P. S.; Huff, J. R. *J. Med. Chem.* **1994**, 37, 3443.
7. Painter, G. R.; Ching, S.; Reynolds, D.; Clair, M. St.; Sadler, B. M.; Elkins, M.; Blum, R.; Dornsife, R.; Livingston, D. J.; Partaledis, J. A.; Pazhanisamy, S.; Tung, R. D.; Tisdale, M. *Drugs Future* **1996**, 21, 347.
8. Kaldor, S. W.; Kalish, V. J.; Davies, J. F.; Shetty, B. V.; Fritz, J. E.; Appelt, K.; Burgess, J. A.; Campanale, K. M.; Chirgadze, N. Y.; Clawson, D. K.; Dressman, B. A.; Hatch, S. D.; Khalil, D. A.; Kosa, M. B.; Lubbehusen, P. P.; Muesing, M. A.; Patick, A. K.; Reich, S. H.; Su, K. S.; Tatlock, J. H. *J. Med. Chem.* **1997**, 40, 3979.
9. Nugiel, D. A.; Jacobs, K.; Corneliuss, L.; Chang, C. H.; Jadhav, P. K.; Holler, E. R.; Klabe, R. M.; Bacheler, L. T.; Cordova, B.; Garber, S.; Reid, C.; Logue, K. A.; Gorey-Feret, L. J.; Lam, G. N.; Erickson-Viitanen, S.; Seitz, S. P. *J. Med. Chem.* **1997**, 40, 1465.
10. Boyer, F. E.; Vara Prasad, J. V.; Domagala, J. M.; Ellsworth, E. L.; Gajda, C.; Hagen, S. E.; Markoski, L. J.; Tait, B. D.; Lunney, E. A.; Palovsky, A.; Ferguson, D.; Graham, N.; Holler, T.; Hupe, D.; Nouhan, C.; Tummino, P. J.; Urumov, A.; Zeikus, E.; Zeikus, G.; Gracheck, S. J.; Sanders, J. M.; VanderRoest, S.; Brodfuehrer, J.; Iyer, K.; Sinz, M.; Gulnik, S. V. *J. Med. Chem.* **2000**, 43, 843.
11. Navia, M. A.; Sato, V. L.; Tung, R. D. *Int. Antivir. News* **1995**, 9, 143.
12. Melnick, M.; Reich, S. H.; Lewis, K. K.; Mitchell, L. J. Jr.; Nguyen, D.; Trippe, A. J.; Dawson, H.; II Davies, J. F.; Appelt, K.; Wu, B. W.; Musick, L.; Gehlhaar, D. K.; Webber, S.; Shetty, B.; Kosa, M.; Kahil, D.; Andrada, D. *J. Med. Chem.* **1996**, 39, 2795.
13. Reich, S. H.; Melnick, M.; Pino, M. J.; Fuhry, M. A.; Trippe, A. J.; Appelt II, K.; Davies, J. F.; Wu, B. W.; Musick, L. *J. Med. Chem.* **1996**, 39, 2781.
14. Reich, S. H.; Melnick, M.; II Davies, J. F.; Appelt, K.; Lewis, K. K.; Fuhry, M. A.; Pino, M.; Trippe, A. J.; Nguyen, D.; Dawson, H.; Wu, B.; Musick, L.; Kosa, M.; Kahil, D.; Webber, S.; Gehlhaar, D. K.; Andrada, D.; Shetty, B. *Proc. Natl. Acad. Sci. U.S.A.* **1995**, 92, 3298.
15. Massa, S.; Di Santo, R.; Mai, A.; Botta, M.; Artico, M.; Panico, S.; Simonetti, G. *Il Farmaco* **1990**, 45, 833.
16. Van Leusen, A. M.; Siderius, H.; Hoogenboom, B. E.; Van Leusen, D. *Tetrahedron Lett.* **1972**, 52, 5337.
17. Ragno, R.; Marshall, G. R.; Di Santo, R.; Costi, R.; Massa, S.; Rompei, R.; Artico, M. *Bioorg. Med. Chem.* **2000**, 8, 1423.
18. Head, R. D.; Smythe, M. L.; Oprea, T. I.; Waller, C. L.; Green, S. M.; Marshall, G. R. *J. Am. Chem. Soc.* **1996**, 118, 3959.
19. Marshall, G. R.; Head, R. D.; Ragno R. *Thermodynamics in Biology*. In Press.
20. Ragno, R.; Head, R. D.; Marshall, G. R. 216th ACS National Meeting 1998, COMP 032.
21. SYBYL™ (Molecular Modeling System); Tripos Associates: 1699 S Hanley Rd, St. Louis, MO 63144, USA.
22. Baroni, M.; Costantino, G.; Cruciani, G.; Riganelli, D.; Valigi, R.; Clementi, S. *Quant. Struct.-Act. Relat.* **1993**, 12, 9.
23. Cramer, R. D. I.; Patterson, D. E.; Bunce, J. D. *J. Am. Chem. Soc.* **1988**, 110, 5959.
24. After the co-crystal structure of AG1132, AG1157 and 1284 with HIV-PR were solved, an inversion of binding mode was observed. Turning from secondary to tertiary amide the carbinol configuration of Agouron's compounds change from S to R when bound to HIV-PR. For this reason we decided to model all the compounds in both the configuration (see ref. 14).
25. Mohamadi, F.; Richards, N. G. J.; Guida, W. C.; Liskamp, R.; Lipton, M.; Caufield, C.; Chang, G.; Hendrickson, T.; Still, W. C. *J. Comput. Chem.* **1990**, 11, 440.
26. Lee, T.; Le, V.-D.; Lim, D.; Lin, Y.-C.; Morris, G. M.; Wong, A. L.; Olson, A. J.; Elder, J. H.; Wong, C.-H. *J. Am. Chem. Soc.* **1999**, 121, 1145.
27. Marcorin, G. L.; Da Ros, T.; Castellano, S.; Stefancich, G.; Bonin, I.; Miertus, S.; Prato, M. *Org. Lett.* **2000**, 2, 3955.
28. Friedman, S. H.; Ganapathi, P. S.; Rubin, Y.; Kenyon, G. L. *J. Med. Chem.* **1998**, 41, 2424.
29. Cramer, C. J.; Truhlar, D. G. *J. Comput. Aided Mol. Des.* **1992**, 6, 629.